PCCP

Accepted Manuscript

ROYAL SOCIETY OF CHEMISTRY

www.rsc.org/pccp

Journal Name

RSCPublishing

ARTICLE

Monitoring hydroquinone/quinone redox cycling by single molecule fluorescence spectroscopy

Cite this: DOI: 10.1039/x0xx00000x

A. Rybina,[a] B. Thaler[b], R. Krämer[b] and D.-P. Herten[a,*]

Received 00th January 2012,
Accepted 00th January 2012

DOI: 10.1039/x0xx00000x

www.rsc.org/

Current research in the field of single-molecule chemistry is increasingly focused on the development of reliable experimental approaches for investigating chemical processes on a molecular level using single-molecule fluorescence spectroscopy (SMFS). Herein, we report on single-molecule observations of the copper(II)/air mediated oxidation of fluorescently labeled hydroquinone-based probe molecules followed by their reduction with cysteine. The redox cycle is signaled by quenching/recovery of fluorescence emission after addition of the oxidant/reductant, respectively. The experiments were realized by immobilizing the probe on a glass cover slide to allow single-molecule observation by means of total-internal-reflection fluorescence microscopy. Besides detection of successful oxidation and reduction events on single probe molecules, individual molecular intensity trajectories revealed dynamic processes and formation of intermediate states upon reaction. For the experimental design presented, we envision further reaction studies of catalytic redox-processes of single hydroquinone-moieties by means of SMFS.

Introduction

An inherent challenge of mechanistic reaction studies in the bulk is addressing alternative and reversible reaction pathways, e.g. as discussed for catalytic oxidation reactions with copper(II)-species.[1,2] Real-time single-molecule fluorescence spectroscopy offers a modern experimental opportunity for the direct observation of individual molecular transformations occurring in complex catalytic reactions, thus delivering a direct insight in sequences of elementary reaction steps and alternative or rare reaction pathways without the need for synchronization.[3-9] Temporal and spatial resolution of these techniques allow for monitoring of single conversion events one by one at individual catalytic sites at the microsecond timescale. For a particular reaction sequence to be observable, the chemical transformation must be signaled by a specific and detectable change in the molecular fluorescence signal. This prerequisite can be achieved by implementing a fluorescent reporter group into the structure of one reaction partner that changes its spectroscopic properties during the reaction.

So far, only few single-molecule studies of redox reactions were carried out mimicking homogeneous conditions.[10-12] Most experiments reported to date have been focusing on a variety of nanoparticles and crystallites.[13-17] An important outcome of these studies is that there exist large differences not only in the catalytic activities among different particles but also among different catalytic sites of a particle. More recently, the application of single-molecule methods has been extended towards reactions of different organometallic compounds also involved in catalytic processes.[18,19] Different approaches and their promising future perspectives have been recently highlighted and discussed by Blum and Cordes.[7]

With the long term objective to extend single-molecule studies also to homogeneous reactions we work on the concept of "pseudo-homogeneous" reactions, where we immobilize individual reactants on microscopy slides in such a way that the reactant is surrounded with solvent molecules and shows minimal interaction with the glass surface. In this context, we have developed surface-immobilized fluorophore-labeled chelating polypyridyl ligands and monitored the reversible formation of individual Cu(II) complexes by fluorescence quenching of the reporter fluorophore.[20,21] In case of a tetradentate complex which is relatively stable towards metal dissociation, the dynamics of fluorescence changes in presence of a reductant at individual sites suggest catalytic Cu(II)/Cu(I) redox cycling, triggered by reduction of Cu(II) and its re-oxidation by dioxygen from air.[11] A different approach – the surface immobilization of the substrate - enabled observation of alternative reaction pathways in epoxidation of single olefin groups signaled by a spectral shift in fluorescence emission of an attached BODIPY reporter.[12]

Herein, we describe single-molecule studies of the redox reaction of surface immobilized hydroquinone-based redox sensors. Various Cu(II) complexes including $[Cu(phen)_2]^{2+}$ (phen = 1,10-phenanthroline) have been reported to mediate

smooth oxidation of hydroquinone to benzoquinone in aerated solution; the overall process is, however, rather complex and mechanistic details remain ambiguous or obscure.[1] A mechanistic study of the bis(phenanthroline)Cu(II) catalyzed oxidation of hydroquinone to benzoquinone in the presence of O_2 has suggested several alternative pathways, possibly even involving operation of more than one mechanism simultaneously. One pathway involves direct oxidation of hydroquinone to semiquinone by one-electron transfer to the Cu(II) complex, followed by conversion of semiquinone to benzoquinone either by O_2-oxidation or redox disproportionation. Another pathway implicates a Cu(II) coordinated hydroquinone anion that reacts with dioxygen, either in a two-electron transfer step or in two subsequent one-electron transfer steps, yielding benzoquinone and H_2O_2 or 2 O^{2-}, respectively.[1] Even for the industrially important diamine-Cu(II) catalyzed oxidative coupling polymerization of 2,6-dimethylphenol in the presence of O_2 (leading to poly(1,4-phenylene ether, widely used as polymer blend Noryl), the mechanism is not entirely elucidated after five decades of mechanistic studies.[2]

We have previously described the redox sensors **1** and **2** that consist of a hydroquinone derivative coupled to rhodamine B (Figure 1a).[22] Upon oxidation by the Cu(II) complex $[Cu(phen)_2]^{2+}$ to the quinone form, we observed quenching of the fluorescence emission. Fluorescence is restored by subsequent regeneration of the hydroquinone form by cysteine reduction. This results encouraged us to prepare an immobilized analog of these redox sensors and monitor reversible hydroquinone/quinone redox transformation catalyzed by $[Cu(phen)_2]^{2+}$ on single-molecule level using total internal reflection microscopy (TIRFM). It should be stressed that in this study we use the rhodamine B as reporter to learn about the reactions of the attached quinone/hydroquinone moiety which is distinct from directly influencing the different redox states of the fluorophore itself as it is done in studies of reducing/oxidizing buffers.[23]

Results and Discussion

Amide coupling reaction between the free secondary amino function of rhodamine B piperazine amide[24] and 2,5-dihydroxyterephtalic acid yielded the novel carboxy-functionalized, rhodamine B labeled hydroquinone **3** (Figure 1a). The properties of **3** are closely related to those of **1** and **2**. On excitation at the absorbance maximum at 566 nm (ε = 81900 $M^{-1}cm^{-1}$) in water, pH 7, **3** displays a strong fluorescence with a maximum at 593 nm. As for **1** and **2**, fluorescence is effectively quenched by hydroquinone-to-quinone oxidation. Fluorescence of the control rhodamine B piperazine amide[24] is unaffected by $[Cu(phen)_2]^{2+}$ or cysteine.[22]

Time-resolved single-molecule studies of **3** require its immobilization on glass cover slides. For immobilization we have converted **3** into its NHS ester **4** (Figure 1a), using the coupling reagent carbonyl diimidazole (CDI). Performing an optimized surface preparation procedure;[25] the slides were amino-functionalized using a mixture of 3-aminopropyl-triethoxysilane (APS) and (3-trimethoxysilylpropyl)-diethylene-triamine (DETA) as linker molecules. We then

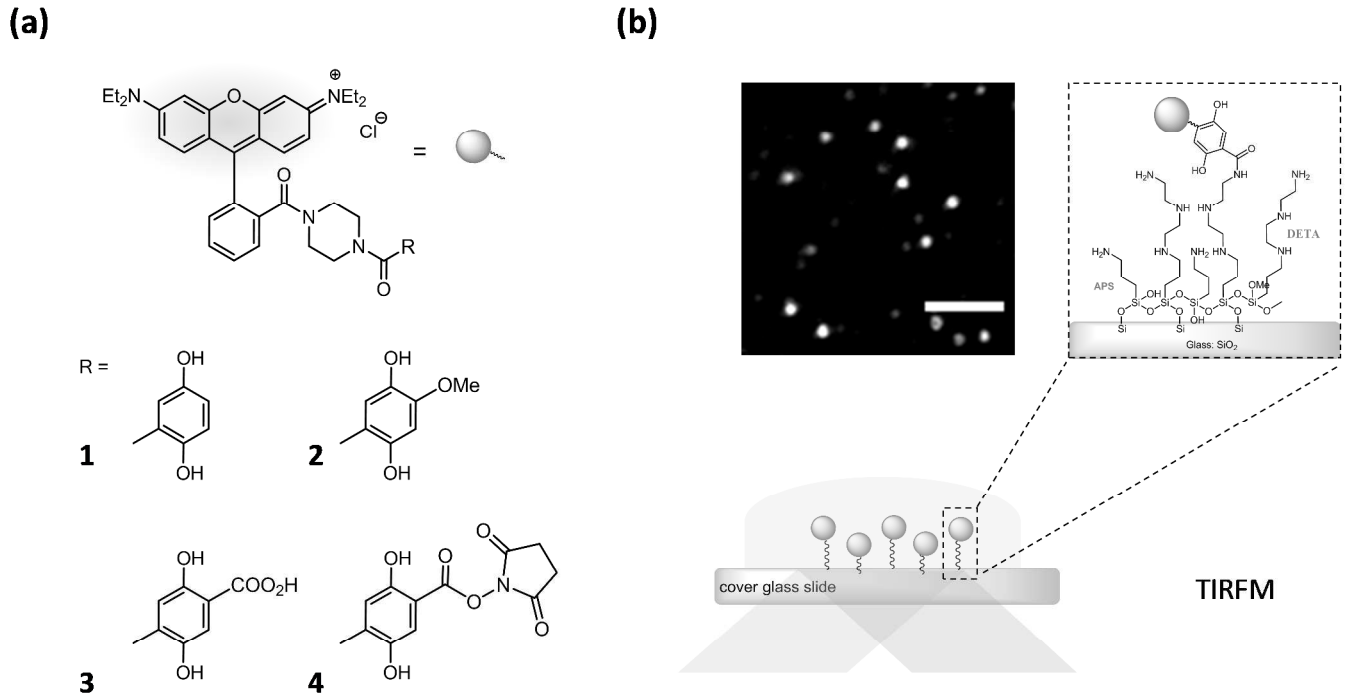

Figure 1. (a) Structures of rhodamine B coupled hydroqinones **1-4**. (b) Scheme of the single molecule experiments: Nanomolar concentrations of the NHS-ester **4** were used for covalent attachment to a glass surface functionalized with APS and DETA (see text). Samples were imaged under TIRF illumination (532 nm, ca. 300 μW) using an emCCD-camera (135.58 ms/frame). Single substrate molecules are visualized as isolated fluorescent spots (scale bar 3 μm).

applied a standard protocol to covalently attach the NHS ester 4 (0.1 nM solution) to the amino-functions at the glass surface (Figure 1b).[26] The samples were studied with total-internal reflection (TIRF) microscopy using cw-laser excitation at 532 nm with a laser power of 300 µW.

For single-molecule experiments we first placed 500 µl 3-(N-morpholino)propanesulfonic acid (MOPS) buffer (10 mM, pH=7.4) on top of the sample. MOPS buffer was chosen because it is a standard buffer for neutral pH which is important due to the pH dependency of the quinine/hydroquinone reaction. In addition, the buffer coordinates Cu(II) ions only very weakly. The redox reaction was then induced by directly adding the reagents to the water droplet while the sample was imaged by an emCCD-camera at a time resolution of 135.58 ms (100 ms exposure time and 35 ms read out time). Data were analyzed by extracting fluorescence intensity transients of 241 single molecules using home built Matlab routines.[12] In the presented experiments, we first induced an oxidation of the hydroquinone substrate by addition of $[Cu(phen)_2]^{2+}$ (2 µM) after 3 s. After 133 s we then induced a reduction of the immobilized probes by addition of cysteine (200 µM) to give a 100 fold molar excess of the reducing agent. Typical examples of single-molecule transients are shown in Figure 2a-f and typical TIRF images reflecting the different states are shown in Figure 2h. For comparison with ensemble data the overall change of the surface fluorescence signal was summed up to form a bulk trace that was corrected for background (Figure 2i). Like in the ensemble studies of **1** we found that the overall intensity drops rapidly after addition of

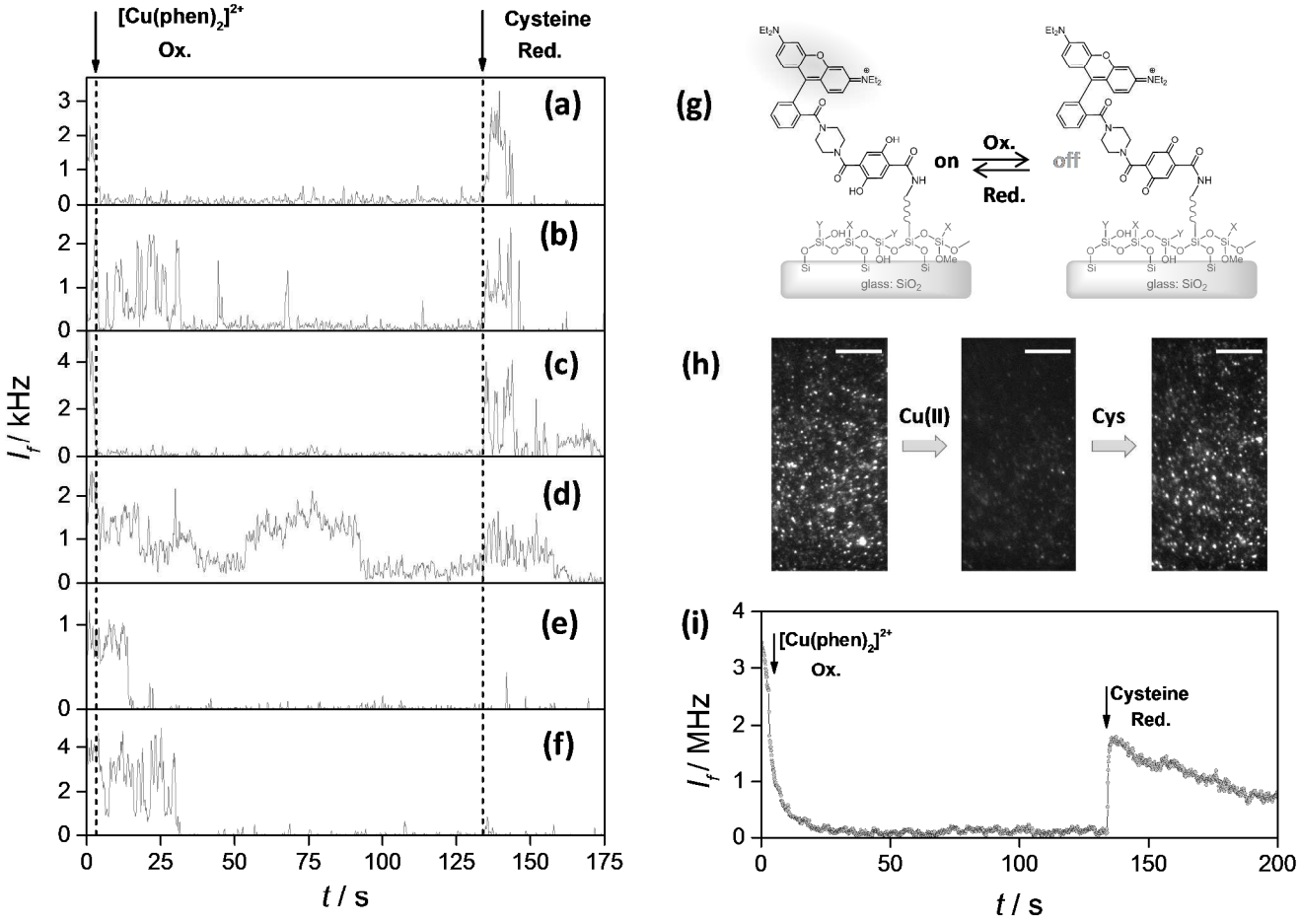

Figure 2. (a)-(f) Typical background corrected single-molecule fluorescence trajectories extracted from the redox experiment on the immobilized substrate (compare to Figure 2) upon addition of the oxidizing catalyst $[Cu(phen)_2]^{2+}$ (2 µM, t = 3 s, red arrow) and the reducing compound cysteine (200 µM, t = 133 s , blue arrow), λ_{ex} = 532 nm (300 µW), emission: 555 - 615 nm, exposure time: 100 ms, frame rate: 7.4 Hz, RT, 10 mM 3-(N-morpholino)propanesulfonic acid (MOPS) buffer, pH=7.4. (g) Reaction scheme of the reversible redox process on a single immobilized substrate molecule (X, Y = DETA and APS linker-moieties). (h) TIRFM micrographs showing different reaction stages in the single-molecule redox experiment. (Each image was obtained by summing up 25 subsequent frames at time points: t=0-3s, 130-133 s and 135-138 s, scale bar 10 µm). (i) Bulk trace obtained upon integration of the fluorescence signal from the surface area 45x22 μm^2, illustrating the overall change of intensity

$[Cu(phen)_2]^{2+}$, most likely due to the catalyzed oxidation of single substrate molecules (Figure 2g). After addition of cysteine, the signal showed an immediate recovery back to 67% of the original intensity. In the single-molecule experiments we found that 57.2% of all molecules (138 out of 241) exhibit a full recovery of fluorescence emission (Figure 2a-d) supporting the notion of previous findings in the ensemble that the oxidation has been fully reversed by addition of cysteine.[22] Some of the molecules, however (exemplified in traces 2e and 2f) appear to remain in quenched or non-fluorescent states, indicating that the immobilized 2,5-bis(carbonyl)substituted hydroquinone can be susceptible to side reactions, like irreversible oxidation.

As mentioned before, most molecules (~57%) show an immediate change of fluorescence emission upon addition $[Cu(phen)_2]^{2+}$ and cysteine (Fig. 2a-f) thereby indicating rapid redox transformations. Strong fluctuations are partly observed either upon oxidation (Figure 2b) or reduction (Figure 2c). Such trajectories might reflect the reversible formation of intermediates, such as the radical semi-quinone structure, as it has been postulated for the $[Cu(phen)_2]^{2+}$ mediated oxidation of hydroquinone in aerobic aqueous conditions.[1] However, similar behavior can be observed in absence of oxidizing and reducing agents pointing towards additional photophysical reactions as frequently observed for many fluorophores (Fig. S1a). Nevertheless, we have to point out that the strong changes in fluorescence emission observed for **4** are most probably mediated by the quinine/hydroquinone moiety as control experiments with rhodamine B don't show any influence by $[Cu(phen)_2]^{2+}$ and cystein (Fig. S1b). A minor part of fluorescence trajectories exhibit variable intensity states (Figure 2d), suggesting several different interactions or structural changes of the substrate affecting its photophysical properties. This behavior indicates non-uniform behavior of the hydroquinone molecules eventually leading to different long lived intermediate or product (quinone) molecules. Yet, the majority of this rather heterogeneous mixture of oxidation products/intermediates recover fluorescence emission upon reduction by cystein, thereby indicating the reversibility of most of the reactions occurring. More detailed analysis of this data along with additional analytical studies might give deeper insights on the underlying reaction pathways. It is noteworthy that 21.2 % of all examined traces (in total 51 of 241) do not show recovery of the fluorescence emission after addition of cysteine (Figure 2e and f). Clearly, these fluorophores have been bleached, potentially due to photodestruction and oxidation reactions. The remaining 21.8 % of all examined single-molecule traces show random signals that could not be attributed to any of the discussed reactions.

Experimental Procedure

Synthesis of 3. Rhodamine B piperazine amide was prepared as described in the literature.[24] **3** was prepared in a two-step procedure, starting with Rhodamine B piperazine amide and 2,5-dihydroxyterephthalic acid, with an overall yield of 20% . 181 mg (0.91 mMol) 2,5-dihydroxyterephthalic acid is dissolved in dry DMF under argon. 345 mg (0.91 mMol) HBTU and 145 µL (1.14 mMol) DIEA are added and the mixture is stirred at room temperature for 30 minutes. 500 mg (0.91 mMol) Rhodamine B piperazine amide are added and the mixture stirred for 15 hours at room temperature. 50 mL water are added and the solution saturated with KCl. The solution is extracted four times with 200 mL chloroform. Chloroform extracts are combined and dried over MgSO4. After filtration, the solvent is evaporated at reduced pressure. The intermediate HBTU amide of **3** (chloride salt) is isolated by column chromatography (silica, chloroform/methanol gradient) in form of a pink solid, and was characterized by ^{1}H NMR, ^{13}C NMR spectroscopy. 20 mg (24 mMol) of the HBTU amide of **3** (chloride salt) are dissolved in 8 mL methanol and 30 mL water and 1 mL conc. HCl added, followed by stirring at room temperature for two hours. The solution is extracted four times with 50 mL dichloromethane. Organic extracts are combined and dried over $MgSO_4$. After filtration, the solvent is evaporated at reduced pressure, yielding the chloride salt of **3** as a pink powder. Yield 15 mg (85%).

Spectroscopic Data of HBTU amide of **3** (chloride salt)

^{1}H NMR: (Methanol-d_4,400 MHz) δ= 1,30 (t, 12 H, J= 7,0 Hz), 3,49 (m, 8 H), 3,68 (q, 8 H, J 7,2 Hz), 6,56 (s br, 1 H), 6,96 (d, 2 H, J = 2,4 Hz), 7,05 (m, 2 H), 7,26 (m, 2 H), 7,32 (s, 1 H), 7,38 (m, 2 H), 7,52 (m, 1 H), 7,70 (d, 1 H, J 7,6 Hz), 7,76 (m, 3 H), 7,78 (d, 1 H, J= 7,6 Hz)ppm.

^{13}C (DEPT): (Methanol-d_4, 100 MHz) δ = 12,9 (CH3,), 47,0 (CH2), 97,4 (CH), 112,0 (CH), 114,9 (Cq), 115,5 (CH), 115,6 (Cq), 115,9 (CH), 118,7 (CH, C28 U. C31), 126,2 (CH, C9), 126,6 (CH, C29 U. C30), 128,7 (Cq, C13), 129,0 (CH), 129,3 (CH), 131,3 (CH), 131,4 (CH), 133,2 (CH), 136,6 (Cq), 139,4 (Cq), 145,7 (Cq), 145,9 (Cq), 148,7 (Cq), 155,7 (Cq), 157,3 (Cq), 159,3 (Cq), 169,6 (Cq), 170,0 (Cq)ppm.

Spectroscopic Data of **3** (chloride salt)

HR Electrospray mass spectrometry: calc. for $[M–Cl]^+$: 691.3132 found 691.3170

UV-Vis (10 µM solution of **3** in water, pH 7): lmax = 566 nm, ε = 81900 M-1cm-1

Fluorescence (10 µM solution of **3** in water, pH 7): lmax = 593 nm

^{1}H NMR: (Methanol-d_4,400 MHz) δ = 1,30 (t, 12 H, J= 6,8 Hz), 3,48 (m, 8 H), 3,68 (q, 8 H, J 6,8 Hz), 6,68 (s, 1 H), 6,95 (s br, 2 H), 7,05 (s br, 2 H), 7,26 (s br, 2 H), 7,32 (s, 1 H), 7,52 (m, 1 H), 7,74 (m, 3 H) ppm.

^{13}C (DEPT): (Methanol-d_4, 100 MHz) δ =12,8 (CH3), 46,9 (CH2), 97,3 (CH), 111,4 (CH), 114,8 (Cq), 115,4 (CH), 117,0 (CH), 127,1 (CH), 128,3 (CH), 128,9 (CH), 131,3 (CH), 131,5 (Cq), 131,8 (Cq), 133,1 (CH), 136,5 (Cq), 146,5 (Cq), / 156,1 (Cq), 156,9 (Cq), 157,1 (Cq), 157,2 (Cq), 159,2 (Cq), 169,5 (Cq), 172,7 (Cq) ppm.

Synthesis of 4. 44 mg (61 mMol) **3** are dissolved in 10 mL dry DMF under argon atmosphere. 9.8 mg (61 µMol) carbonyl diimidazole are added and the reaction mixture stirred for one hour at 60°C. A solution of 7.0 mg (61 µMol) N-hydroxysuccinimide in 1 mL dry DMF is added dropwise and the reaction mixture stirred at 60°C for 15 hours. The

solvent is removed under removed pressure, yielding **4** in form of a pink powder.
The compounds **3** and **4** were characterized by ^{1}H NMR, ^{13}C NMR spectroscopy, HR Electrospray mass spectrometry, UV-Vis spectrometry and Fluorescence spectroscopy.

Spectroscopic Data of **4** (chloride salt)
HR Electrospray mass spectrometry: m/z calc. for $[M\text{-}Cl]^{+}$: 705,3288 found 705,3318
^{1}H NMR: (Chloroform-d_3, 600 MHz) δ = 1,24 (s br, 12 H, H16), 2,57 (s, 8 H, H28), 2,99 (m, 8 H, H17 u. H18), 3,51 (s br, 8 H, H15), 6,67 (s br, 2 H, H2), 6,85 (s br, 2 H, H4), 7,10 (m, 2 H, H5), 7,11 (s, 1 H, H25), 7,15 (s, 1 H, H22), 7,51 (m, 2 H, H10 u. Hil), 8,15 (m, 1 H, H9 u. H12) ppm.
^{13}C (DEPT). (Chloroform-d_3, 150 MHz) δ = 12,4 (CH3, C16), 29,6 (CH2, C28), 46,0 (CH2, C15), 96,2 (CH, C2), 110,9 (CH, C25), 113,8 (CH, C4), 113,6 (Cq, C6), 119,7 (CH, C5), 127,8 (CH, C 1 U. Cli), 129,9 (CH, C22), 130,0 (Cq, C20), 130,1 (Cq, C23), 130,3 (CH, C9 U. C12), 133,8 (Cq, C13), 150,8 (Cq, C7), 152,2 (Cq, C8), 155,5 (Cq, C21), 155,5 (Cq, Cl), 157,6 (Cq, C24), 157,6 (Cq, C3),174,3 (Cq, C14, C19 U. C26), 174,3 (Cq, C27) ppm.

Bulk experiments. Fluorescence spectra and intensity were measured with Varian Cary Eclipse Fluorimeter, using PMMA Macro Cuvettes (Semadeni) and quartz glass cuvettes (Suprasil©, from Hellma, Müllheim). UV-Vis spectra were obtained at a Varian Cary 100 Bio UV/Vis spectral photometer, using PMMA Macro Cuvettes (Semadeni). Electrospray mass spectra were recorded at a Waters Q-TOF ultima mass spectrometer. Cyclovoltammetry was performed on a Potentiostat 263A (EG&G Princeton Applied Research) using ECHEM Software.
Surface immobilization of 3. The amino-silane functionalized glass surfaces were prepared according to the optimized surface coating protocol presented by Metwalli *et al*.[25] The microscopic cover glass slides were first cleaned by immersion in 2.5 M NaOH solution for 24 hours followed by sonification in water for 10 min and a subsequent immersion in 0.1 M HCL-solution for 15 minutes. After sonification in water for 10 min and immersion in methanol for 5 minutes, silanization of the clean glass slides was carried out by dip coating for 15 minutes into a 1 % aqueous aminosilane solution containing a mixture of 3-aminopropyl-triethoxysilane (APS) and 3-trimethoxysilylpropyl-diethylene-triamine (DETA) in a ratio 1:5. The glass slides were washed in methanol for 5 minutes and in water for 10 minutes, dried with a spin coater and heated at 110°C for 20 minutes to give coated surfaces, stored under vacuum before further treatment. For the covalent substrate attachment, 500 µl of PBS buffer (pH 7.4) were placed onto the surface and mixed with 10 µl of a 10 nM solution of **4** (in DMF) upon careful addition. After 3 hours reaction time, the solution was removed and the surface several times washed with PBS buffer.
Single-molecule experiments. Single-molecule experiments were performed on a custom built total-internal-reflection-fluorescence (TIRF) microscope according to the setup description published previously[12] with a band pass filter BrightLine HC 585/60 placed in the detection channel for the green fluorescence.
In the single-molecule experiments the redox reaction was initiated by first adding 10 µL of the $[Cu(phen)_2]^{2+}$ solution (0.1 mM, in dd water) into the solvent droplet on the prepared surface. After oxidation, 10 µL of cysteine solution (10 mM, in dd water) were added to perform the subsequent reduction respectively. For single-molecule data analysis, individual traces were extracted, corrected for background and visually inspected as previously reported.[12]

Conclusions

In conclusion, we designed a fluorescent redox-sensor for monitoring reversible redox reactions on the electrochemically active hydroquinone derivative by means of SMFS. A reversible reaction sequence could be achieved performing Cu(II)/air mediated oxidation followed by reduction with cysteine, signaled by quenching and subsequent recovery of molecular emission of the chromophoric moiety Rhodamine B. Implementation of probe immobilization and TIRF-microscopy in our experiments allowed for the real time observation of the complete redox-cycles of single molecules revealing heterogeneities of molecular reaction behavior. The distinguishable single-molecule trajectories presumably reflect formation of multiple intermediate states and dynamic processes along individual reaction pathways eventually leading to a heterogeneous distribution of different long-lived intermediates and products most of which are returned to the substrate after addition of the reducing agent. Thus, we speculate that the different species forming the heterogeneous product mixture after oxidation remain connected via a dynamic equilibrium. It should also be noted that quinone/hydroquinone systems can show strong quenching as exemplified here for rhodamine B making them less attractive in the context of self-healing dyes despite their interesting redox properties.[26,27]
For future experiments, we envision a detailed investigation of individual molecular reaction trajectories as well as characterization of molecular intermediate state formation along with support by analytical techniques, offering new perspectives for a deeper understanding of chemical redox processes. Due to the reversible nature of the reaction, the controlled on/off switching may have potential for applications requiring the chemical control of emissive and dark molecular states, like in super-resolution fluorescence microscopy, or for enabling new ways of multiplexing in fluorescence microscopy.[28,29] However, for such applications, the dynamic switching between the oxidized and reduced states still needs to be established and reliably defined by experimental parameters. Nevertheless, the advantage of the probe is given by its flexibility towards structural tuning of its electrochemical redox-potential by variation of residues attached to the hydroquinone unit thus allowing for combinations with different redox-systems.

Acknowledgements

We gratefully acknowledge financial support by the Deutsche Forschungsgemeinschaft (DFG, SFB 623 and EXC81). We thank Anton Kurz and Kristin Grußmayer for their software support and Alexander Kiel, Andrji Mokhir and Arndt Sprödefeld for fruitful discussions. We also thank Daniel Hack, Lena Hahn and Sven Wiesner for their contributions during their practical in our lab.

Notes and references

[a] Universität Heidelberg, Cellnetworks Cluster & Physikalisch-Chemisches Institut, Im Neuenheimer Feld 267, 69120 Heidelberg, Germany.
[b] Universität Heidelberg Anorganisch-Chemisches Institut, Im Neuenheimer Feld 270, 69120 Heidelberg, Germany.

Corresponding Author

*Fax: +49-6221 54-51444, email: dirk-peter.herten@urz.uni-heidelberg.de

(1) S. Mandal, S, N.H. Kazmi, L.M. Sayre, Ligand dependence in the copper-catalyzed oxidation of hydroquinones. *Arch. Biochem. Biophys.* 2005, **435**, 21–31.

(2) P. Gamez, S. Gupta,J. Reedijk, Copper-catalyzed oxidative coupling of 2,6-dimethylphenol: A radicalar or an ionic polymerization? *C. R. Chimie* 2007**, 10**, 295–304.

(3) M. B. J. Roeffaers, G. de Cremer,H. Uji-i, B. Muls,B. F. Sels,P. A. Jacobs, F. C. de Schryver, D. E. De Vos, J. Hofkens, Single-molecule fluorescence spectroscopy in (bio)catalysis. *Proc. Nat. Acad. Sci. USA* 2007**, 104**, 12603–12609.

(4) G. de Cremer, B. F. Sels, D. E. de Vos, J. Hofkens, M. B. J. Roeffaers, Fluorescence micro(spectro)scopy as a tool to study catalytic materials in action. *Chem. Soc. Rev.* 2010, **39**, 4703- 4717.

(5) P. Chen, X. Zhou, H. Shen, N. M. Andoy, E. Choudhary, K.-S. Han, G. Liu, W. Meng, Single-molecule fluorescence imaging of nanocatalytic processes. *Chem. Soc. Rev*. 2010, **39**, 4560- 4570.

(6) T. Tachikawa, T. Majima, Single-Molecule, Single-Particle Approaches for Exploring the Structure and Kinetics of Nanocatalysts*. Langmuir* 2012, **28**, 8933–8943.

(7) T. Cordes, S. A. Blum, Opportunities and challenges in single-molecule and single-particle fluorescence microscopy for mechanistic studies of chemical reactions. *Nature Chem.* 2013**, 5**, 993–999.

(8) K. P. F. Janssen, G. de Cremer, R. K. Neely, A. V. Kubarev, J. van Loon, J. A. Martens, D. E. de Vos, M. B. J. Roeffaers, J. Hofkens, Single molecule methods for the study of catalysis: from enzymes to heterogeneous catalysts. *Chem. Soc. Rev.* 2014, **43**, 990–1006.

(9) S. A. Blum, Location change method for imaging chemical reactivity and catalysis with single-molecule and -particle fluorescence microscopy. *Phys. Chem. Chem. Phys.* 2014, *Advance article*, DOI: 10.1039/C4CP00353E.

(10) R. Ameloot, M. Roeffaers, M. Baruah, G. de Cremer, B. Sels, D. de Vos, J. Hofkens, Towards direct monitoring of discrete events in a catalytic cycle at the single molecule level. *Photochem. Photobiol. Sci.* 2009**, 8**, 453-456.

(11) A. Sprödefeld, A. Kiel, D.-P. Herten, R. Krämer, Monitoring Cu 2+ -Binding to a DNA-Clip-phen Conjugate and Metal-centered Redox Processes by a Fluorescent Reporter Group. *Z. anorg. allg. Chem.* 2013**, 639**, 1636–1639.

(12) A. Rybina, C. Lang, M. Wirtz, K. Grußmayer, A. Kurz, F. Maier, A. Schmitt, O. Trapp, G. Jung, D.-P. Herten, Distinguishing Alternative Reaction Pathways by Single-Molecule Fluorescence Spectroscopy. *Angew. Chem., Int. Ed.* 2013**, 52**, 6322–6325.

(13) G. de Cremer, M. B. J. Roeffaers, E. Bartholomeeusen, K. Lin, P. Dedecker, P. P. Pescarmona, P. A. Jacobs, D. E. de Vos, J. Hofkens, B. F. Sels, High-Resolution Single-Turnover Mapping Reveals Intraparticle Diffusion Limitation in Ti-MCM-41-Catalyzed Epoxidation, *Angew. Chem., Int. Ed*. 2010, **49**, 908–911.

(14) X. Zhou, W. Xu, G. Liu, D. Panda, P. Chen, P. Size-Dependent Catalytic Activity and Dynamics of Gold Nanoparticles at the Single-Molecule Level. *J. Am. Chem. Soc.* 2010**, 132**, 138–146.

(15) X. Zhou, N. M. Andoy, G. Liu, E. Choudhary, K.-S. Han, H. Shen, P. Chen, Quantitative super-resolution imaging uncovers reactivity patterns on single nanocatalysts. *Nature Nanotech.* 2012, **7**, 237–241.

(16) T. Tachikawa, S. Yamashita, T. Majima, Probing Photocatalytic Active Sites on a Single Titanosilicate Zeolite with a Redox-Responsive Fluorescent Dye. *Angew. Chem., Int. Ed*. 2010, **49**, 432–435.

(17) T. Tachikawa, S. Yamashita, T. Majima, Evidence for Crystal-Face-Dependent TiO2 Photocatalysis from Single-Molecule Imaging and Kinetic Analysis. *J. Am. Chem. Soc.* 2011, **133**, 7197–7204.

(18) N. M. Esfandiari, Y. Wang, J. Y. Bass, S. A. Blum, Deconvoluting Subensemble Chemical Reaction Kinetics of Platinum–Sulfur Ligand Exchange Detected with Single-Molecule Fluorescence Microscopy. *Inorg. Chem.* 2011, **50**, 9201–9203.

(19) E. M. Hensle, S. A. Blum, Phase Separation Polymerization of Dicyclopentadiene Characterized by In

Operando Fluorescence Microscopy. *J. Am. Chem. Soc.* 2013, **135**, 12324–12328.

(20) A. Kiel, J. Kovacs, A. Mokhir, R. Krämer, D.-P. Herten, Direct Monitoring of Formation and Dissociation of Individual Metal Complexes by Single-Molecule Fluorescence Spectroscopy. *Angew. Chem., Int. Ed.* 2007, **46**, 3363–3366.

(21) D. Brox, A. Kiel, S. J. Wörner, M. Pernpointner, P. Comba, B. Martin, D.-P. Herten, M. Sauer, Ensemble and Single-Molecule Studies on Fluorescence Quenching in Transition Metal Bipyridine-Complexes. *PLoS ONE* 2013, **8**, e58049.

(22) R. M. Kierat, B. M. Thaler, R. Krämer, A fluorescent redox sensor with tunable oxidation potential. *Bioorg. Med. Chem. Lett.* 2010, **20**, 1457–1459.

(23) J. Vogelsang, R. Kasper, C. Steinhauer, B. Person, M. Heilemann, M. Sauer, P. Tinnefeld, A Reducing and Oxidizing System Minimizes Photobleaching and Blinking of Fluorescent Dyes. *Angew. Chem. Int. Ed.* 2008, **47**, 5465–5469.

(23) T. Nguyen, M. B. Francis, Practical Synthetic Route to Functionalized Rhodamine Dyes. *Org. Lett.* 2003, **5**, 3245–3248.

(24) E. Metwalli, D. Haines, O. Becker, S. Conzone, C. G. Pantano, Surface characterizations of mono-, di-, and tri-aminosilane treated glass substrates. *J. Colloid Interface Sci.* 2006, **298**, 825–831.

(25) G. T. Hermanson, *Bioconjugate techniques;* Academic Press: Amsterdam, 2008.

(26) R.B. Altman, D.S. Terry, Z. Zhou, Q. Zheng, P. Geggier, R.A. Kolster, Y. Zhao, J.A. Javitch, J.D. Warren, S.C. Blanchard, Cyanine fluorophore derivatives with enhanced photostability. *Nature Methods* 2012, **9**, 68-73.

(27) P. Tinnefeld, T. Cordes, 'Self-healing dyes' – intramolecular stabilization of organic fluorophores. *Nature Methods* 2012, **9,** 426-427.

(28) D. Brox, M. Schwering, J. Engelhardt, D.-P. Herten, Reversible Chemical Reactions for Single-Color Multiplexing Microscopy. *ChemPhysChem* 2014*, Early view,* DOI: 10.1002/cphc.201402012.

(29) M. Schwering, A. Kiel, A. Kurz, K. Lymperopoulos, A. Sprödefeld, R. Krämer, D.-P. Herten, Far-Field Nanoscopy with Reversible Chemical Reactions. *Angew. Chem., Int. Ed.* 2011, **50** (13), 2940–2945.

Graphical abstract for the table of contents